

Efficient light amplification in low gain materials due to a photonic band edge effect

L. Ondič^{1,2,3,*} and I. Pelant¹

¹ Institute of Physics, Academy of Sciences of the Czech Republic, v.v.i., Cukrovarnická 10, 162 53, Prague 6, Czech Republic

² Faculty of Mathematics and Physics, Charles University, Ke Karlovu 3, 121 16 Prague 2, Czech Republic

³ IPCMS–DON Unité Mixte, UMR 7504, CNRS–ULP, 23 rue du Loess, BP 43, 67034 Strasbourg Cedex 2, France

* ondic@fzu.cz

Abstract: One of the possibilities of increasing optical gain of a light emitting source is by embedding it into a photonic crystal (PhC). If the properties of the PhC are tuned so that the emission wavelength of the light source with gain falls close to the photonic band edge of the PhC, then due to low group velocity of the light modes near the band edge caused by many multiple reflections of light on the photonic structure, the stimulated emission can be significantly enhanced. Here, we perform simulation of the photonic band edge effect on the light intensity of spectrally broad source interacting with a diamond PhC with low optical gain. We show that even for the case of low gain, up to 10-fold increase of light intensity output can be obtained for the two-dimensional PhC consisting of only 19 periodic layers of infinitely high diamond rods ordered into a square lattice. Moreover, considering the experimentally feasible structure composed of diamond rods of finite height - PhC slab - we show that the gain enhancement, even if reduced compared to the ideal case of infinite rods, still remains relatively high. For this particular structure, we show that up to 3.5-fold enhancement of light intensity can be achieved.

© 2012 Optical Society of America

OCIS codes: (050.5298) Photonic crystals; (310.6628) Subwavelength structures, nanostructures; (310.6805) Theory and design.

References and links

1. E. Yablonovitch, "Inhibited spontaneous emission in solid-state physics and electronics," *Phys. Rev. Lett.* **58**, 2059–2062 (1987).
2. J. D. Joannopoulos, S. G. Johnson, J. N. Winn, and R. D. Meade, *Photonic Crystals: Molding the Flow of Light* (Princeton University Press, 2008).
3. J. C. Knight, J. Broeng, T. A. Birks, and P. St. J. Russell, "Photonic band gap guidance in optical fibers," *Science* **282**, 1476–1478 (1998).
4. H.-G. Park, C. J. Barrelet, Y. Wu, B. Tian, F. Qian, and C. M. Lieber, "A wavelength-selective photonic-crystal waveguide coupled to a nanowire light source," *Nat. Photon.* **2**, 622–626 (2008).
5. S. Noda, M. Fujita, and T. Asano, "Spontaneous-emission control by photonic crystals and nanocavities," *Nat. Photon.* **1**, 449–458 (2007).
6. D. Taillaert, P. Bienstman, and R. Baets, "Compact efficient broadband grating coupler for silicon-on-insulator waveguides," *Opt. Lett.* **29**, 2749–2751 (2004).

7. S. Fan, P. R. Villeneuve, J. D. Joannopoulos, and E. F. Schubert, "High extraction efficiency of spontaneous emission from slabs of photonic crystals," *Phys. Rev. Lett.* **78**, 3294–3297 (1997).
8. M. Fujita, S. Takahashi, Y. Tanaka, T. Asano, and S. Noda, "Simultaneous inhibition and redistribution of spontaneous light emission in photonic crystals," *Science* **308**, 1296–1298 (2005).
9. J. J. Wierer, A. David, and M. M. Megens, "III-nitride photonic-crystal light-emitting diodes with high extraction efficiency," *Nat. Photon.* **3**, 163–169 (2009).
10. T. F. Krauss, "Slow light in photonic crystal waveguides," *J. Phys. D: Appl. Phys.* **40**, 2666–2670 (2007).
11. J. Grgic, J. Pedersen, S. Xiao, and N. Mortensen, "Group index limitations in slow-light photonic crystals," *Photon. Nano.* **8**, 56–61 (2010).
12. J. P. Dowling, M. Scalora, M. J. Bloemer, and C. M. Bowden, "The photonic band-edge laser: A new approach to gain enhancement," *J. Appl. Phys.* **75**, 1896 (1994).
13. Y. A. Vlasov, K. Luterova, I. Pelant, B. Honerlage, and V. N. Astratov, "Enhancement of optical gain of semiconductors embedded in three-dimensional photonic crystals," *Appl. Phys. Lett.* **71**, 1616 (1997).
14. M. Nomura, S. Iwamoto, A. Tadaechanurat, Y. Ota, N. Kumagai, and Y. Arakawa, "Photonic band-edge micro lasers with quantum dot gain," *Opt. Express* **17**, 640–648 (2009).
15. K. Sakoda, "Enhanced light amplification due to group-velocity anomaly peculiar to two- and three-dimensional photonic crystals," *Opt. Express* **4**, 167–176 (1999).
16. D. Wiersma, "The smallest random laser," *Nature* **406**, 132–135 (2000).
17. J. Andreasen, A. A. Asatryan, L. C. Botten, M. A. Byrne, H. Cao, L. Ge, L. Labonté, P. Sebbah, A. D. Stone, H. E. Türeci, and C. Vanneste, "Modes of random lasers," *Adv. Opt. Photon.* **3**, 88–127 (2011).
18. S. Ossicini, L. Pavesi, and F. Priolo, *Light Emitting Silicon for Microphotonics* (Springer, 2003).
19. H. Chen, J. H. Shin, and P. M. Fauchet, "Optical gain in silicon nanocrystal waveguides," in *Silicon Nanophotonics: Basic Principles, Present Status and Perspectives*, L. Khriachtchev, ed. (World Scientific Publishing, 2009), pp. 89–117.
20. K. Dohnalová, K. Židek, L. Ondič, K. Kůsová, O. Cibulka, and I. Pelant, "Optical gain at the F-band of oxidized silicon nanocrystals," *J. Phys. D: Appl. Phys.* **42**, 135102 (2009).
21. A. M. Zaitsev, *Optical Properties of Diamond: A Data Handbook* (Springer, 2001).
22. I. Aharonovich, A. D. Greentree, and S. Praver, "Diamond photonics," *Nature Photon.* **5**, 397–405 (2011).
23. A. Kromka, B. Rezek, Z. Remes, M. Michalka, M. Ledinsky, J. Zemek, J. Potmesil, and M. Vanecek, "Formation of continuous nanocrystalline diamond layers on glass and silicon at low temperatures," *Chem. Vap. Deposition* **14**, 181–186 (2008).
24. S. Tomljenovic-Hanic, M. J. Steel, C. M. de Sterke, and J. Salzman, "Diamond based photonic crystal microcavities," *Opt. Express* **14**, 3556–3562 (2006).
25. J. W. Baldwin, M. Zalalutdinov, T. Feygelson, J. E. Butler, and B. H. Houston, "Fabrication of short-wavelength photonic crystals in wide-band-gap nanocrystalline diamond films," *J. Vac. Sci. Technol. B* **24**, 50 (2006).
26. C. F. Wang, R. Hanson, D. D. Awschalom, E. L. Hu, T. Feygelson, J. Yang, and J. E. Butler, "Fabrication and characterization of two-dimensional photonic crystal microcavities in nanocrystalline diamond," *Appl. Phys. Lett.* **91**, 201112 (2007).
27. L. Ondič, K. Dohnalová, M. Ledinský, A. Kromka, O. Babchenko, and B. Rezek, "Effective extraction of photoluminescence from a diamond layer with a photonic crystal," *ACS Nano* **5**, 346–350 (2011).
28. S. G. Johnson and J. D. Joannopoulos, "Block-iterative frequency-domain methods for Maxwell's equations in a planewave basis," *Opt. Express* **8**, 173–190 (2001).
29. A. F. Oskooi, D. Roundy, M. Ibanescu, P. Bermel, J. D. Joannopoulos, and S. G. Johnson, "Meep: A flexible free-software package for electromagnetic simulations by the FDTD method," *Comput. Phys. Commun.* **181**, 687–702 (2010).
30. S. G. Johnson, S. Fan, P. R. Villeneuve, J. D. Joannopoulos, and L. A. Kolodziejski, "Guided modes in photonic crystal slabs," *Phys. Rev. B* **60**, 5751–5758 (1999).
31. W. M. Robertson, G. Arjavalingam, R. D. Meade, K. D. Brommer, A. M. Rappe, and J. D. Joannopoulos, "Measurement of photonic band structure in a two-dimensional periodic dielectric array," *Phys. Rev. Lett.* **68**, 2023–2026 (1992).
32. K. Sakoda, "Symmetry, degeneracy, and uncoupled modes in two-dimensional photonic lattices," *Phys. Rev. B* **52**, 7982–7986 (1995).
33. N. Ganesh, W. Zhang, P. C. Mathias, E. Chow, J. A. N. T. Soares, V. Malyarchuk, A. D. Smith, and B. T. Cunningham, "Enhanced fluorescence emission from quantum dots on a photonic crystal surface," *Nature Nanotech.* **2**, 515–520 (2007).
34. E. Chow, S. Y. Lin, S. G. Johnson, P. R. Villeneuve, J. D. Joannopoulos, J. R. Wendt, G. A. Vawter, W. Zubrzycki, H. Hou, and A. Alleman, "Three-dimensional control of light in a two-dimensional photonic crystal slab," *Nature* **407**, 983–986 (2000).
35. R. Sprik, B. A. van Tiggelen, and A. Lagendijk, "Optical emission in periodic dielectrics," *Europhys. Lett.* **35**, 265 (1996).
36. A. Asatryan, S. Fabre, K. Busch, R. McPhedran, L. Botten, M. de Sterke, and N. A. Nicorovici, "Two-dimensional local density of states in two-dimensional photonic crystals," *Opt. Express* **8**, 191–196 (2001).

37. A. F. Koenderink, M. Kafesaki, C. M. Soukoulis, and V. Sandoghdar, "Spontaneous emission rates of dipoles in photonic crystal membranes," *JOSA B* **23**, 1196–1206 (2006).
38. Q. Wang, S. Stobbe, and P. Lodahl, "Mapping the local density of optical states of a photonic crystal with single quantum dots," *Phys. Rev. Lett.* **107**, 167404 (2011).

1. Introduction

Photonic crystals (PhCs) are materials possessing a periodicity in refractive index which offer control of the way light propagates in the medium [1, 2]. They are extensively studied because of their interesting optical properties which can be used to prepare photonic waveguides [3, 4], cavities [5], couplers [6] or outcouplers [7–9] of light and other optical devices with dimensions comparable or smaller than the wavelengths of light that they are designed for. Further devices may also take advantage of slow-light modes [10, 11], namely the ability to enhance stimulated emission due to the effects occurring near the photonic band edge. Near the band edge, the group velocity of the photon propagating through the structure is strongly reduced due to a large number of multiple reflections within the PhC. In case when a material in the state of population inversion is present this effect may lead to enhancement of effective optical gain [12]. This idea was already experimentally realized for semiconductor quantum dots (QDs) exhibiting relatively high values of optical gain [13, 14]. It was also shown that in two-dimensional (2D) PhCs with only several periodic layers the so-called group velocity anomaly may affect the stimulated emission more strongly than the photonic band edge effect itself [15]. Let us note here that even in disordered gain materials the principle of multiple light scattering may also lead to the light amplification and lasing - the so-called random lasing (for a review, see [16, 17]). Nevertheless, in this article, we will focus only on periodic structures.

The principal feasibility of enhancing optical gain via PhCs appears, naturally, even more attractive when considering active materials with low optical gain coefficient, i.e. materials with the optical gain coefficient lower than is the typical gain coefficient for direct band gap semiconductors (where it amounts to several hundreds up to thousands of cm^{-1}). The driving force behind the present study stems from the state-of-the-art of silicon photonics, where the crucial issue of a suitable light source - a silicon-based laser - has not been satisfactorily solved up to now. Luminescent silicon nanocrystals (SiNCs) seem to be one of the possible solutions [18], however, their optical gain is rather low [19, 20]. Therefore, SiNCs (the active laser medium) incorporated into the PhC serving as the optical resonator may be a solution.

In order to obtain effective gain enhancement, a material possessing both high refractive index and low optical losses should be used. Moreover, it should possess high thermal conductivity in order to withstand high power pumping, and also good optical quality is required - diamond therefore seems to be one of good candidates [21, 22]. Compared to other materials (Si, InP, etc.) generally used for a PhC preparation, it has a wide electronic band gap thus possessing very low losses in the visible spectral region. This is important property as the SiNCs shine at around 600–800 nm. Growth of nanocrystalline diamond (NCD) layers [23] represent viable approach as compared with expensive bulk diamond. Simulations studying the possibility of realizing cavity in NCD have already been performed [24] and nano-patterning of NCD layers has already been well developed [25–27].

In this article, we aim to demonstrate the photonic band edge effect by means of computer simulation of the transmission and gain-influenced transmission spectra (gain spectra) in two types of PhC with 2D planar periodicity in dielectric constant. One of them has an infinite height, the so-called 2D PhC and the other one features a finite height, the so-called PhC slab. Compared to other authors [12, 15], we consider the optical gain to be very low and, moreover, we take into account the finite height of real-life PhC which also reduces the enhancement in comparison to the infinitely high 2D PhC. The results are applicable to any material with low

optical gain, distributed uniformly in a suitable PhC.

2. Results and discussion

2.1. Simulation in general

Photonic band diagrams were computed using the Plane-wave-expansion technique [28].

Transmission and gain spectra were simulated using Finite-Difference Time-Domain (FDTD) method [29] considering a spectrally broad pulse as a light source.

In simulation, the system is described by a complex dielectric constant $\varepsilon = \varepsilon_1 + i\varepsilon_2$, which varies periodically with the position vector \mathbf{r} . However, in spectroscopy in the visible region a complex refractive index $N = n + i\kappa$ is more commonly used, where the real part n indicates phase velocity of light in the medium and its value is ~ 2.4 for diamond. The imaginary part κ describes, depending on its sign, the effect of absorption loss or gain when the electromagnetic wave propagates through the material.

When κ is negative, the intensity of light propagating within material will exponentially increase. Therefore, optical gain can be in first approximation implemented by considering the imaginary part of the dielectric constant to be negative. A gain saturation will be neglected in the model describing the case when the intensity of propagating light is relatively low. One can imagine the simulation to be equivalent to a situation when gain active semiconductor QDs (e.g., SiNCs) are uniformly distributed inside a dielectric medium (PhC).

As we wish to apply this approach to low gain material we will consider relatively low optical gain coefficient value $\alpha \sim -126 \text{ cm}^{-1}$ at a (vacuum) wavelength of 500 nm. This is equivalent to $\kappa \sim -0.0005$ based on the relation $\alpha = 2\kappa \frac{\omega}{c}$. Finally, we get $\varepsilon_2 = 2n\kappa \sim -0.0024$.

As we are interested in describing the physical effect of the gain enhancement, the simulation will be performed at the spectrally broad region keeping in mind that in reality the gain material emission is spectrally narrow. And due to the spectrally narrow gain, we can neglect the spectral dependence of refractive index and gain in the simulation.

2.2. 2D PhC

We start with investigation of the 2D PhC consisting of infinitely long dielectric rods with refractive index $n = 2.4$ ordered into a lattice with the square symmetry surrounded by air. Radius of rods is $r = 0.3a$, where a is a lattice constant. All the units used within this article are expressed in units of the lattice constant a . This PhC has a complete band gap for TM modes (modes odd with respect to the mirror plane $z = 0$ perpendicular to the rods) [30]. Experimentally, this structure can be realized in the case that the incident light beam does not "see" edges of the sample and its wavefront is not affected by the finite height of the sample [31].

Photonic band diagrams for the two experimentally accessible crystal directions of this structure, the Γ -X and Γ -M, are shown in Fig. 1(a) and 1(b), respectively. The insets show an electric field patterns of the modes as computed for each band at $k_x = 0.3$, $k_y = 0$ in (a) and $k_x = 0.3$, $k_y = 0.3$ in (b) where k_x , k_y are the in-plane components of the wavevector given by relation $\mathbf{k}_{\parallel} = \frac{2\pi}{a}(k_x, k_y)$. Border of each rod is depicted with an open circle. One can clearly recognize the wave fronts of propagating light waves with direction of propagation marked by black arrows. The first, second and fourth (not shown) field patterns are symmetric with respect to the mirror plane depicted by solid black line and therefore these modes can be excited by the incoming plane wave coming from outside in the indicated direction because it possesses the similar mirror symmetry [31, 32]. On the other hand, modes of the third photonic band (dashed line) are asymmetric with respect to the mirror plane and therefore cannot be excited by the incident plane wave. This effect is reproduced in the transmission spectra obtained for 19 periods of rods having refractive index N purely real (no losses/gain), as plotted on the right-hand side of the band diagrams in Fig. 1, and it can be clearly recognized that for example in the case

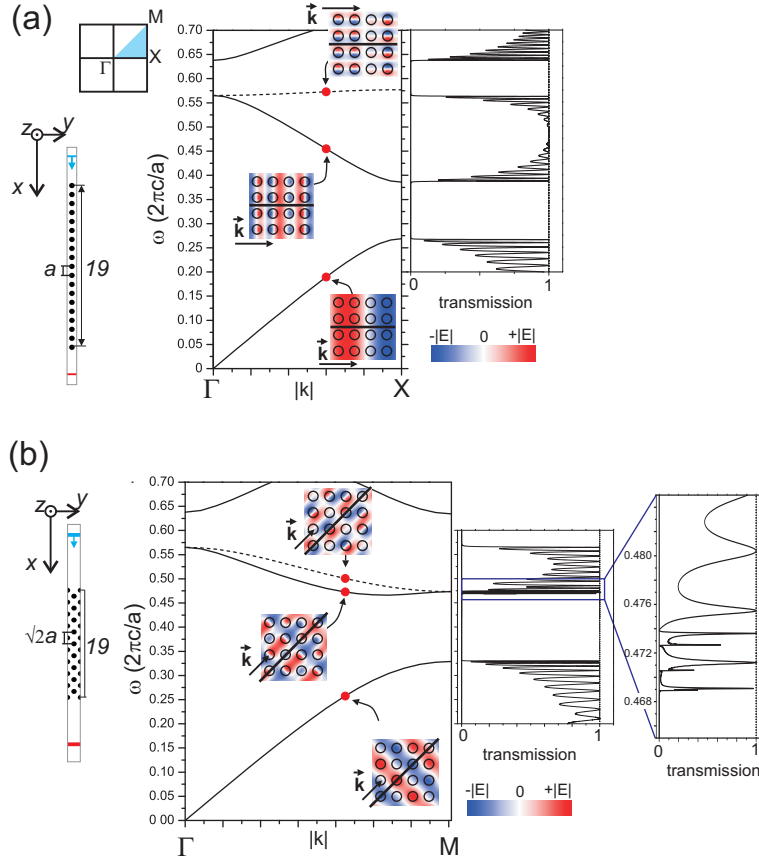


Fig. 1. Photonic diagrams for TM modes in the Γ -X (a) and Γ -M (b) directions of the square array of infinitely high diamond rods (2D PhC) with radius $r = 0.3a$, where a is the lattice constant. The insets show the electric field (parallel to the rods, z -direction) patterns of the modes for each band at the wavevector marked by the red spot. Bands whose mode patterns are symmetric and asymmetric with respect to the mirror plane (a black line in each field pattern) are plotted with solid and dashed line, respectively. The left-hand side of the photonic band diagram in each panel shows the computational domain used for computation of the transmission spectra shown on the right-hand side of the band diagram. The blue and red rectangles represent a light source and a detector, respectively.

of transmission spectrum computed for the Γ -X direction, the bottom edge of the second band gap is defined by the top of the second band at Γ point and not by the top of the third band at X point (Fig. 1(a)).

The 2D computational domains used for the simulation of transmission spectra are shown in the left part of Fig. 1(a) and 1(b) for the Γ -X and Γ -M directions, respectively. The domain includes the material under study (19 rods layers). On the top and bottom surfaces of the computational domain, we impose the Perfectly Matched Layer absorbing boundary conditions. For the remaining two surfaces, we impose a Bloch periodic boundary condition on the electric fields [29]. We generate an incident plane wave from the line source (blue rectangle) with a wavefront parallel to the rods and detect the transmitted flux (red rectangle).

On the basis of the shape of the photonic bands we see that the states with low group velocity ($v_g \sim \frac{\partial \omega}{\partial k}$) are mostly formed near the points of high symmetry and for them the high enhance-

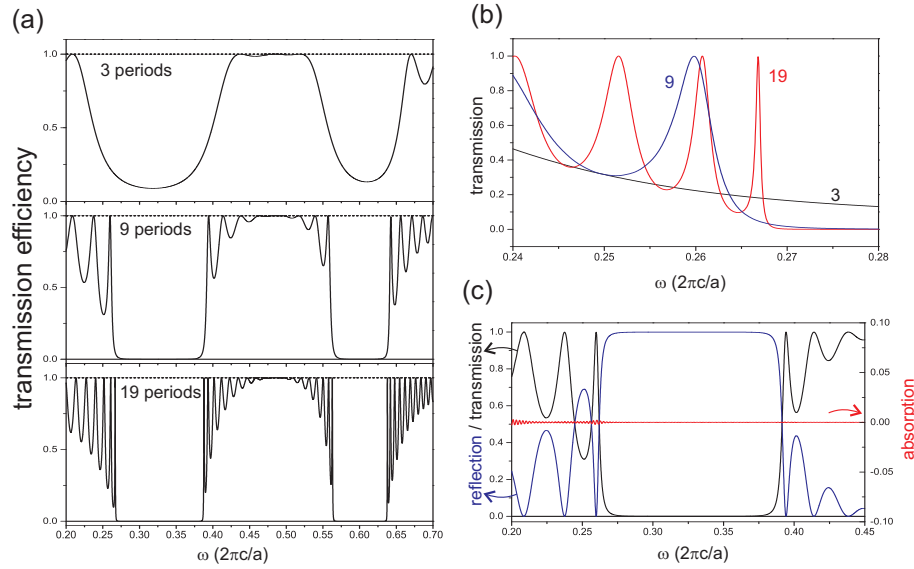


Fig. 2. (a) Transmission spectra of the 2D PhC in the Γ -X direction simulated considering 3, 9 and 19 lattice periods of infinite diamond columns with the lattice constant a . (b) Detail of the transmission spectra - formation of photonic states near the band edge with increasing number of lattice periods. (c) Transmission (T) and reflection (R) spectra of the PhC with 9 lattice periods demonstrating the correctness of the FDTD simulation. The red curve shows the absorption (A) calculated by the formula $A=1-T-R$.

ment of light intensity is expected in the case the optical gain is present. Moreover it is worth noticing that around the frequency of 0.46 in Γ -M direction (Fig. 1(b)) we obtained relatively wide frequency range with a small group velocity (photonic band with very low slope) - the so-called group velocity anomaly region [15] which, as we will see, gives raise to high gain enhancement. The singular shape of the transmission curve in this frequency region (right-hand side of Fig. 1(b)) is due to the convex shape of the band. The photonic band gap is well reproduced in the transmission spectra computed for the structure composed of 19 layers of diamond rods and therefore this structure will be also considered in gain simulations.

The formation of band gap and band edge states with increasing number of layers is plotted in Fig. 2(a) and in detail in Fig. 2(b). The correctness of FDTD simulation is demonstrated in Fig. 2(c) where the transmission and reflection curves are depicted together with the appropriate absorption given by the relation (unity - transmission - reflection). In a non-absorbing medium, this relation should be equal to zero which is in our case fulfilled.

As the next step we introduce the optical gain into the rods ($N = 2.4 - i0.0005$). In this case the incident pulse triggers the stimulated emission in the PhC and the amplified transmitted flux (gain spectrum) is detected. Let us note here that also the intensity of modes reflected on the PhC is increased, however for the sake of clarity we do not plot them.

Gain-influenced transmission spectra for the Γ -X and Γ -M directions are shown in Fig. 3(a) and (b), respectively. The red horizontal curve depicts increased intensity after a single light pass along the given direction, simulated with the refractive index $N = 1 - i0.0005$ in the position of rods and $N = 1$ elsewhere. Its value is ~ 1.017 (1.013) for the Γ -X (Γ -M) crystal direction which means that light intensity was increased only by $\sim 1.7\%$ (1.3%) compared to the reference signal intensity. The values are nearly equal to unity mainly due to low optical gain of our material. On the other hand, the transmitted light intensity is considerably enhanced

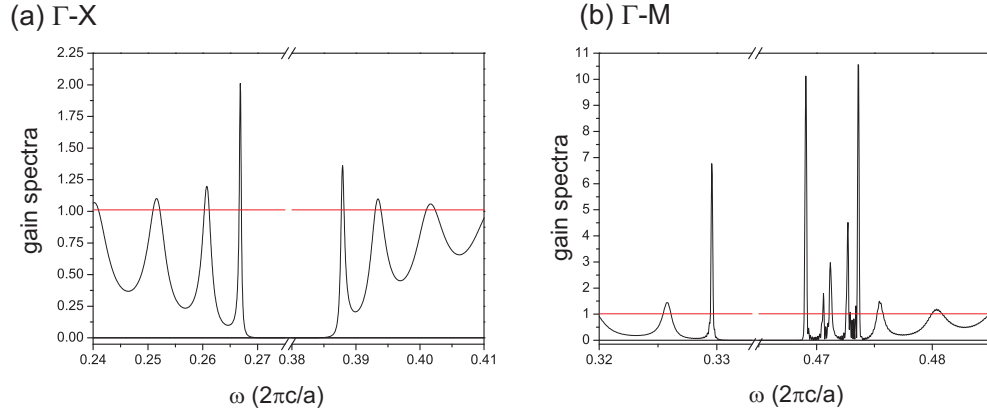


Fig. 3. Gain-influenced transmission spectra (black curve) computed for the TM polarized plane wave incident in the Γ -X (a) and Γ -M (b) crystal directions of the square array of 19 layers of infinitely high diamond rods possessing optical gain. The red horizontal line depicts the single pass light amplification when the periodicity is not present.

Table 1. Fraction of electric field energy confined in the rods computed for the mode at the band edge.

	X-point		M-point	
	2D PhC	PhC slab	2D PhC	PhC slab
band 1	0.88	0.67	0.95	0.75
band 2	0.56	0.56	0.75	0.75

when it propagates through the PhC with the same value of optical gain. For the Γ -X crystal direction, the enhancement is up to 2-fold compared to the reference signal at frequencies of light coupled to the states near the photonic band edge. Even higher increase of transmitted intensity is observed for the Γ -M crystal direction compared to the Γ -X, where three main peaks with the enhancement efficiency from ~ 6 to ~ 10 arise due to photonic band edge effect and due to the group velocity anomaly. The reason for the large intensity enhancement can be readily understood from the intensity amplitude amplification factor derived by Sakoda in [15] which depends on the following four factors. It is inversely proportional to the group velocity of the mode, and thus intensity of light propagating in modes with low group velocity is expected to be greatly increased. Next it holds that the more the mode energy is confined in the active material (rods in our case) the higher the enhancement can be expected. The fraction of the electric field energy confined in rods computed for the modes at the X and M points of the Brillouin zone, given as a ratio of mode energy concentrated in rods and total mode energy, is summarized in Table 1. Lastly, the higher the frequency of the mode the higher the amplification factor. All the above mentioned factors together contribute to the final computed gain spectrum. Nevertheless, it would be unrealistic to expect extremely large output intensity enhancement because the amplification factor scales linearly with the gain coefficient, and thus the anticipated low value of gain keeps the enhancement within moderate limits.

2.3. PhC slab

As a photonic crystal slab we consider a structure consisting of dielectric rods with finite height ($h = 2a$), surrounded by air, and having the same square symmetry and planar dimensions as the 2D PhC discussed in previous section. This structure can be realized experimentally, e.g.

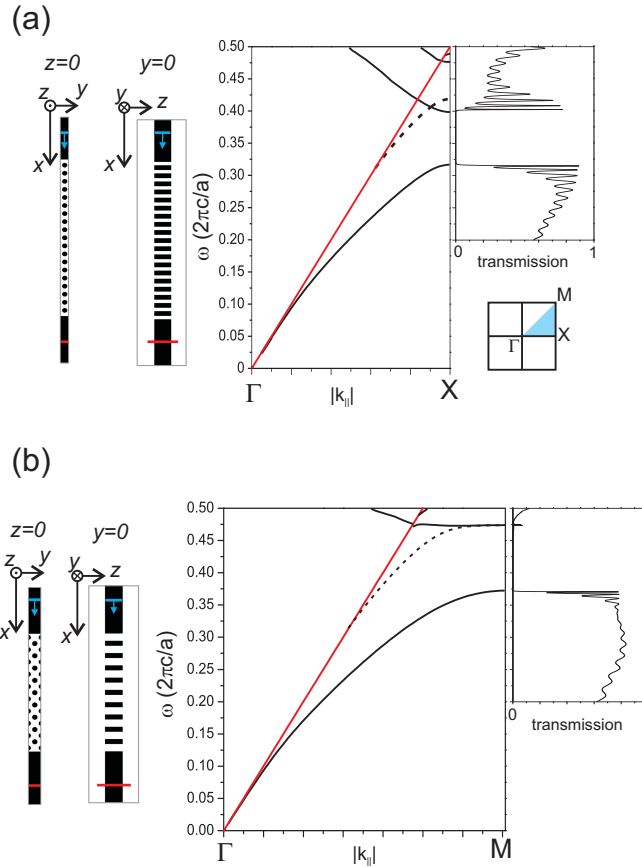


Fig. 4. Projected photonic band diagrams for TM modes in the Γ -X (a) and Γ -M (b) crystal directions of the PhC slab consisting of a square array of diamond rods with radius $r = 0.3a$ and height $h = 2a$, where a is a lattice constant. Modes that are symmetric (asymmetric) with respect to the mirror plane parallel to the direction of mode propagation are plotted with black solid (dashed) lines. The air lightline is depicted with the red line. On the left side of each panel, a computational domain is depicted (a top-view and a side-view) used for simulation of transmission spectra plotted on the right side of each panel. Blue rectangles represent a source of TM polarized light incident in the relevant direction for 19 layers of rods. Red rectangles represent detector plane. Origin of the coordinate system is in the middle of the computational domain.

by using a substrate with very low refractive index ([33] - nanoglass with refractive index of 1.17) or even by patterning the low index substrate in the same manner as the PhC (extending the rods into the substrate) [34]. Then photonic properties of such a structure will only slightly differ from the one we are investigating here.

Projected photonic band diagrams in the Γ -X and Γ -M symmetry directions of our PhC slab for TM-like modes are shown in Fig. 4(a) and 4(b), respectively. Modes that are positioned below the lightline (red line) are confined within the PhC. Strictly speaking, there is no longer any photonic band gap in TM-like modes, however, modes of the second band (marked by dashed line) are asymmetric (not shown) with respect to the mirror plane parallel to the direction of light propagation. Similarly to the previous case of the 2D PhC, the asymmetric modes will not be excited by the incident TM polarized wave and thus photonic band gap actually opens

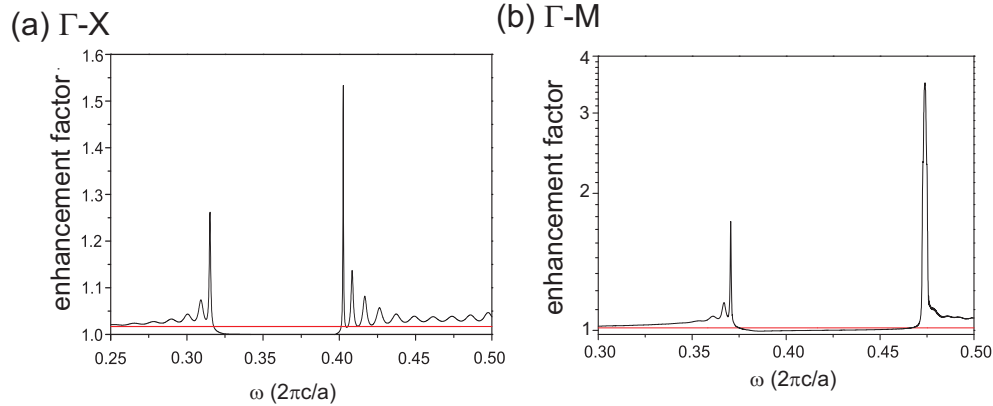


Fig. 5. Photon flux enhancement spectra (black curve) in the Γ -X (a) and Γ -M (b) crystal directions of the PhC slab depicted in Fig. 4, computed as a ratio of the gain-influenced and ordinary transmission spectra. The red horizontal line depicts the single pass enhancement.

for light incident along the Γ -X or Γ -M directions.

Transmission spectra were computed using 3D computational domain. A top and side view of the domain with the PhC slab consisting of 19 layers of rods are shown in the left part of Fig. 4(a) and 4(b) for the Γ -X and Γ -M directions, respectively. On the two surfaces of the computational domain parallel to the xz -plane, we impose a Bloch periodic boundary condition on the electric fields. For the remaining four surfaces of the computational domain, we impose the Perfectly Matched Layer absorbing boundary conditions [29]. Light emitted from the source positioned in the uncorrugated part of the diamond layer (blue rectangle) is at first coupled to the guided modes of the layer, then it couples to the PhC and afterwards couples back again to the uncorrugated layer where the flux guided (transmitted) through the PhC is computed (red rectangle). In order to stay consistent with the previous section, we use the term transmitted signal (transmission spectra) in the sense of the flux guided within the PhC and/or the uncorrugated layer. Transmission spectra of the PhC were normalized by the transmission spectra computed for only the uncorrugated layer without PhC and thus contains also information about the efficiency of guided modes coupling between the layer and the PhC.

Photonic states formed near the band edge can be clearly recognized in transmission spectra shown in Fig. 4 at the right-hand side of each photonic band diagram. Sharp peaks occur near the top of the first band and bottom of the third band in both investigated crystal directions. In the case of the Γ -M direction, only two peaks with very low transmission (~ 0.07) occur around the edge of the third band which happens due to the shape of this band below the lightline where the region of nearly zero group velocity is formed. Even for guided modes, the transmission is lower than unity, which happens due to the losses/reflections introduced during the light coupling to (from) the PhC. On the other hand, modes positioned above the lightline are not purely guided modes and can radiate to air as they propagate within the PhC [7], which explains why the transmission efficiency of modes above the lightline decreases.

A relevant parameter describing enhancement of the transmitted signal through the PhC slab with gain compared to the one without, given by the ratio of gain-influenced (not shown) to ordinary transmission spectra, is plotted in Fig. 5(a) and 5(b) for the Γ -X and Γ -M directions, respectively. The red curve depicts the single pass intensity amplification simulated in such a way that the gain regions are introduced into the uncorrugated layer on the same positions as the rods are distributed over the PhC; due to the low optical gain its value is nearly equal to unity. Thus we can directly read that we obtained up to ~ 1.5 -fold enhancement of light intensity in

the Γ -X crystal direction due to the band edge effect compared to the single pass enhancement despite the finite height of the PhC. In the case of the Γ -M direction, the intensity amplification amounts up to 1.7-fold near the band edge of the first band at point M, and even up to 3.5-fold near the band edge of the third band, again due to the group velocity anomaly.

Results of our simulation show that the enhancement of optical gain occurs always near the band edge and is even higher when a region of group velocity anomaly is present there. As it was shown, the existence of the complete optical band gap is not a necessary condition for obtaining the enhancement. On the other hand, it is very important to adjust dimensions of the PhC based on the refractive index of the material so that the emission spectrum of the gain material overlaps with modes possessing very low group velocity.

Comparison of the results of the two different PhC structures show that the incident light amplification is in the case of the PhC slab lower than in the case of the 2D PhC, which obviously arises from the different nature of these structures, as reflected in the shape of photonic bands (thus the group velocity). Next, due to the finite height of the PhC slab, the mode is extended into air in the vertical z-direction and less mode energy is concentrated in the rods than in the case of the 2D PhC (for comparison see Table. 1). Nevertheless, the enhancement factor in the PhC slab is still much higher than the value of the single pass enhancement suggesting that this approach may be applicable when constructing optical resonators for materials with low optical gain coefficient.

Let us note here that the complementary description of light amplification enhancement due to the photonic band edge effect is possible via the physical quantity called local density of optical states (LDOS) [35]. The LDOS determines the dynamics of radiation sources embedded at a particular position in a PhC. Computation results for the 2D PhC composed of infinitely high rods [36] or the PhC membranes [37] are consistent with results of our simulation. Namely, the LDOS is strongly enhanced for the band edge modes compared to other modes of different frequencies. Moreover, spatial variation of the LDOS is consistent with the electric energy spatial distribution of these modes shown in Table 1. The same effect of enhanced LDOS at the band edges was recently determined experimentally from the decay times of luminescence of QDs embedded in the PhC membranes [38].

3. Conclusions

We demonstrated, by means of a computer simulation, the enhancement of light amplification in a material with low optical gain with the aid of 2D photonic structures. We showed that by introducing the periodicity into the refractive index of the active material, the intensity of light propagating through the structure composed of only 19 periodic layers can be increased by factor varying from 1.5 up to 10. The enhancement arises from the photonic band edge effect and the highest values were obtained when this effect is combined with the group velocity anomaly regime. Comparison of the 2D PhC (infinite height) and PhC slab revealed that both these structure can take the advantage from the photonic band edge effect. For the diamond PhC slab, which is experimentally feasible structure, we obtained up to 3.5-fold enhancement of the optical gain (for the case of 19 periodic layers), which we believe may be useful when constructing optical resonators for the low gain materials operating in the visible region.

Acknowledgments

This work was supported by the Centrum MSMT (Grant No. LC510), GAAV (Grant No. IAA101120804), GAAV (Grant No. KJB100100903), GAUK (Grant No. 73910), Grant SVV-2011-261306, the Institutional Research Plan (Grant No. AV0Z 10100521).